Sensors and Materials, Vol. 38, No. 4 (2026) 1925–1940
MYU Tokyo

S & M 4416

Development of Hybrid Energy Storage System Considering Techno-economic Optimization by Advanced Signal Decomposition for Wind Power Smoothing

Muhammad Nouman Shahzad,[1,2] Obaid ur Rahman,[1,2]
Hsiung-Cheng Lin,[3*] and Ling-Ling Li[1,2]

[1]State Key Laboratory of Intelligent Power Distribution Equipment and System, Hebei University of Technology, Tianjin 300401, China
[2]Key Laboratory of Electromagnetic Field and Electrical Apparatus Reliability of Hebei Province, Hebei University of Technology, Tianjin 300401, China
[3]Department of Electronic Engineering, National Chin-Yi University of Technology. Taichung 41170, Taiwan.

(Received November 10, 2025; accepted December 8, 2025)

Keywords: hybrid energy storage system, wind power fluctuations, complete ensemble empirical mode decomposition, techno-economic analysis, capacity optimization, power allocation

The grid stability threatened by the inherent variability of wind power generation creates a critical need for effective mitigation strategies. To resolve this issue, we aim to develop a battery-supercapacitor hybrid energy storage system (HESS) that integrates an advanced power allocation strategy with a comprehensive techno-economic model to minimize the levelized storage cost. A power-sharing method based on improved complete ensemble empirical mode decomposition with adaptive noise (ICEEMDAN) and Hilbert transform is introduced to optimally decompose fluctuating wind power, allocating high-frequency transients to the supercapacitor and low-frequency components to the battery. The economic model then incorporates the battery capacity status along with battery degradation modelling by reducing battery stress and maintaining the depth of discharge (*DOD*) primarily within a moderate 0.4–0.6 range. Compared with three existing schemes, i.e., EEMD, CEEMDAN, and ICEEMDAN, the proposed ICEEMDAN-based strategy achieves the most cost-effective configuration with a total annualized cost of 172.25 k CNY. Cost reductions are approximately 9.4% compared with the CEEMDAN-based scheme (190.10 k CNY) and 17.7% compared with the EEMD-based scheme (209.16 k CNY). This verifies that the best techno-economic performance can be achieved by optimally balancing power smoothing efficacy with battery longevity and overall system cost.

1. Introduction

The global push for decarbonization is accelerating the integration of renewable sources like wind power. However, the inherent intermittency of wind generation creates grid stability

*Corresponding author: e-mail: hclin@ncut.edu.tw
https://doi.org/10.18494/SAM6013

ISSN 0914-4935
https://myukk.org/

challenges, making energy storage system (ESS) development critical. While hybrid energy storage system (HESS) architectures combining high-energy batteries with high-power supercapacitors offer a technically superior solution for smoothing power fluctuations, their widespread adoption is hindered by economic uncertainties. The high capital investment and complex trade-offs between component sizing, degradation, and lifetime performance make the cost-of-ownership issue highly essential especially for project feasibility and investor confidence.[1,2]

The levelized cost of storage (LCOS) for a HESS is not seen as a simple function of power rating but a complex system operational outcome instead. Although power allocation control between batteries and supercapacitors may directly govern battery usage patterns, the high-frequency battery cycles and deep depth of discharge (*DOD*) accelerate degradation, leading to a shorter lifespan and higher replacement costs.[3] Conversely, an overly conservative power-splitting strategy may necessitate a larger, more expensive supercapacitor. Therefore, the core economic challenge is how to develop a co-optimization framework. In other words, the optimal capacity sizing and the corresponding optimal power-splitting control law to minimize the total lifetime cost should be simultaneously determined.[4]

Existing approaches to HESS optimization often treat the technical and economic problems separately. Numerous power allocation strategies have been proposed, ranging from simple filters like low-pass filtering (LPF) and frequency-domain approaches like the discrete Fourier transform (DFT) to more advanced, adaptive decomposition techniques such as wavelet transforms, empirical mode decomposition (EMD), and its variants (VMD and CEEMDAN).[5–7] While the above methods may improve the quality of power smoothing, their direct impact on lifetime costs, particularly in terms of battery degradation, is frequently oversimplified. For this reason, technical performance metrics over a comprehensive techno-economic analysis should be prioritized to resolve this issue.

However, existing signal processing techniques for HESS power allocation have not led to sufficient economic benefits. For example, an adaptive framework using k-means clustering, weighted filtering, and improved complete ensemble empirical mode decomposition with adaptive noise (ICEEMDAN)–Hilbert analysis worked well for optimal power splitting through smoothing power fluctuations and optimizing power distribution. Nevertheless, a critical question remains: does this technical superiority deliver tangible economic benefits?

Accordingly, this study develops an ESS control strategy for a wind–storage hybrid system on the basis of time–frequency spectrum analysis and capacity constraints, enabling accurate charge–discharge control under real operating conditions. While HESS typically faces higher complexity owing to coordinating battery and supercapacitor operation, the proposed ICEEMDAN–Hilbert decomposition simplifies this process. By automatically separating wind power into frequency-specific components, the method enables a rule-based power split that eliminates the need for complex real-time control loops. Supercapacitors exhibit a comparatively high unit energy cost, but the proposed frequency-driven control strategy minimizes their required energy capacity by ensuring that they handle only short-duration, high-frequency transients. The rain flow counting method is applied to *DOD* for the pattern life. Considering the investment, operation and maintenance (O&M), recovery, and penalty costs associated with

wind power fluctuations, an optimization model with the objective function is introduced to minimize the annualized comprehensive cost. This is achieved by using the IBM ILOG CPLEX Optimization Studio (CPLEX) optimizer. The economic feasibility of the optimized capacity configuration is then analyzed to achieve efficient and cost-effective coordination between wind energy and ESSs.

2. Power Allocation Framework

The inherently low energy density of supercapacitors is mitigated by restricting their operation to the high-frequency transients identified via ICEEMDAN decomposition. Consequently, as the battery exclusively manages long-duration energy requirements, the supercapacitor's limited storage capacity does not constrain overall system performance. In this section, we summarize the signal-processing framework used to generate the battery and supercapacitor power profiles.[8]

2.1 Overview of the signal processing approach

The proposed power allocation framework employs an adaptive decomposition algorithm that dynamically distributes fluctuating wind power between battery and supercapacitor units. The proposed ICEEMDAN–Hilbert framework simplifies the sophisticated control typically required for HESSs by generating frequency-separated intrinsic mode functions (IMFs). This enables a direct, rule-based power allocation where high-frequency components are mapped to the supercapacitor and low-frequency components to the battery, thereby substantially reducing management complexity. For its practical implementation, the strategy relies on real-time sensor technologies. High-resolution measurements of wind power, current/voltage, and state-of-charge (*SOC*) provide the essential data stream for the signal decomposition and transient detection. The reliability and accuracy of these sensors are therefore crucial as they enable the precise power allocation that ensures stable operation, maintains the target battery *DOD* between 0.4 and 0.6, and achieves the presented techno-economic optimization.

2.2 Key processing steps

The power profiles for the battery $P_{bat}(t)$ and supercapacitor $P_{sc}(t)$ are generated through the following sequence of steps:

1. Scenario selection: A representative, high-variability day is selected from a full year of wind farm data using the k-means clustering algorithm. The analysis is based on a realistic and challenging operational scenario.
2. Pre-smoothing: The raw wind power signal $P_{wind}(t)$ is processed using a novel weighted filter that dynamically combines a moving average filter (MAF) and an anti-pulse interference average filter (AIAF). This step generates a stable grid reference power $P_{grid}(t)$. The required compensation power for HESS $P_{hess}(t)$ is then derived as

$$P_{hess}(t) = P_{grid}(t) - P_{wind}(t). \tag{1}$$

3. Adaptive decomposition: The $P_{hess}(t)$ signal is decomposed using the ICEEMDAN algorithm. The complex signal is adaptively decomposed into a set of IMFs ranging from high-frequency to low-frequency components.
4. Hilbert spectral analysis: To prevent the well-known issue of negative instantaneous frequencies in Hilbert-based analysis, the signal is first processed with ICEEMDAN. This decomposition generates mono-component IMFs with reduced mode mixing, which ensures physically meaningful instantaneous frequency estimates. Consequently, the stability and reliability of the subsequent power-sharing decisions are significantly improved.
5. Optimal power split: On the basis of the Hilbert spectrum, the IMFs are allocated to the storage components. High-frequency, low-energy IMFs are assigned to the supercapacitor $P_{sc}(t)$, capitalizing on its rapid response and high-power density. The low-frequency, high-energy IMFs (including the residual) are assigned to the battery $P_{bat}(t)$, leveraging its high energy density for sustained charging and discharging. The complete layout of the entire power allocation framework, outlining the sequential process from data input to the final power split, is illustrated in Fig. 1.

The final outputs of this framework are the time-series data for $P_{bat}(t)$ and $P_{sc}(t)$, which define the operational duty cycles for the battery and supercapacitor, respectively. These profiles are the primary inputs for the techno-economic model described in the following section.

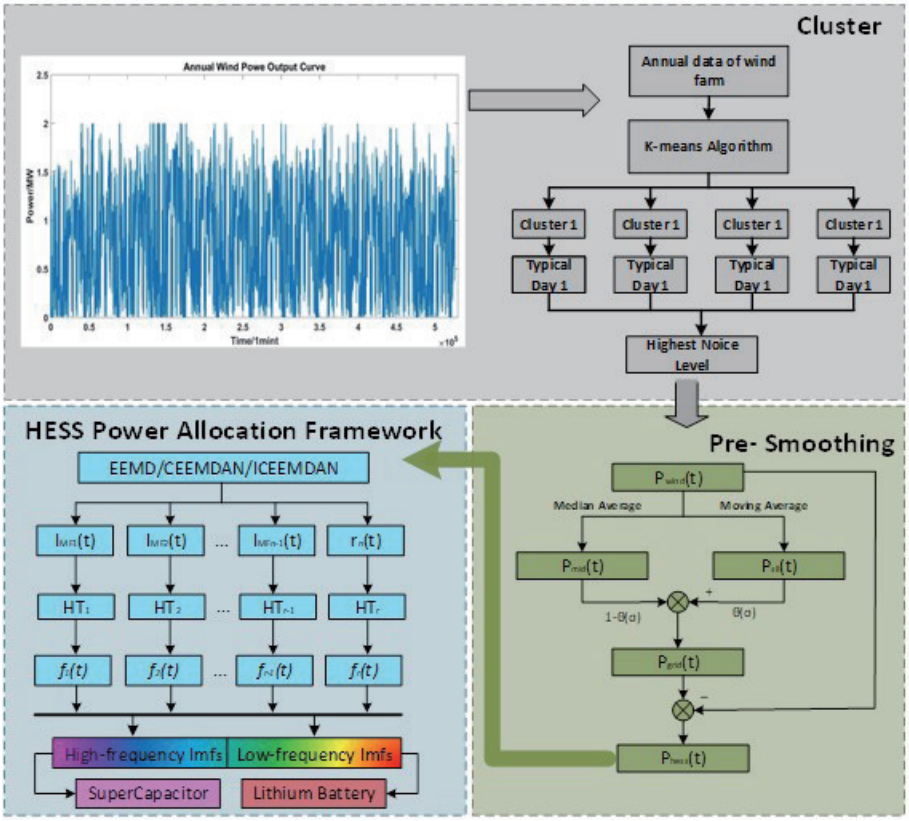

Fig. 1. (Color online) Diagram of power allocation framework.

3. Economic Analysis Model of HESS

Considering power coverage and economic cost, we combine lithium-ion batteries and supercapacitors, two complementary energy storage components, to form a HESS.[9]

3.1 Practical capacity adjustment of HESS components

The nominal power and energy capacities of the HESS are constrained by practical system factors such as depth-of-discharge limits, converter efficiency, thermal derating, and long-term performance degradation.[10] The power (P_p) and energy (E_p) capacities and are calculated as

$$P_p = P_{nom} \times (1 + \alpha_P), \tag{2}$$

$$E_p = E_{nom} \times (1 + \alpha_E), \tag{3}$$

where α_P and α_E represent the power and energy oversizing factors, and P_{nom} and E_{nom} the nominal power and energy, respectively.

In this study, for the lithium-ion battery, we set α_E = 0.4–0 and α_P = 0.2–0. For the supercapacitor, we set α_E = 0.2–0.3 and α_P = 0.15–0.25.[11]

3.2 Battery life estimation by rain-flow counting

The rain flow counting method, initially developed by Matsuishi and Endo for material fatigue analysis, is employed to characterize energy storage system degradation.[12] It establishes a relationship between the *DOD* and the number of cycles.[13] The frequency-based power split also mitigates voltage imbalance by ensuring that the battery handles slow, energy-intensive variations while the supercapacitor manages fast transients within a narrow *SOC* window. This approach maintains each device within its stable voltage range, thereby reducing mismatch and preventing excessive voltage drift. *DOD*, defined as the ratio of discharged capacity to rated capacity in a cycle, profoundly impacts battery longevity. A full cycle constitutes a complete charge and discharge process (e.g., from SOC_1 to SOC_2 and back to SOC_1), whereas a half-cycle represents a single charge or discharge segment (e.g., SOC_1 to SOC_2). *DOD* is expressed as

$$DOD = \left| SOC_1 - SOC_2 \right|. \tag{4}$$

The rain flow counting algorithm is applied to the battery's *SOC* profile to identify individual charge–discharge cycles. The procedure, as illustrated in Fig. 2, is described as follows.

1. Data preparation: The time-series *SOC* data is rotated 90 degrees clockwise, metaphorically representing the data as a pagoda roof from which rain will flow.
2. Flow initiation: The analysis begins at a peak or trough point 1. The "rain flow" continues downward until it encounters a point of greater magnitude than its point of origin.

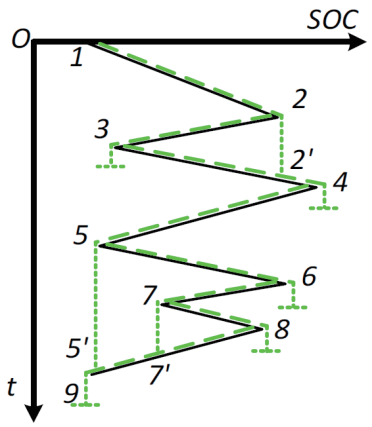

Fig. 2. (Color online) Diagram of rain flow counting method.

3. Flow termination: The flow also terminates if it intercepts a flow path from a previous, higher-level peak or trough. Each termination identifies a complete cycle (e.g., cycle 2-3-2' in Fig. 2).
4. Cycle extraction: By iterating this process, all full and half-cycles within the data are extracted (e.g., cycles 2-3-2', 7-8-7', and 5-6-5').

The output of this method is a distribution of cycles by *DOD*. This distribution is then used in conjunction with an empirical battery degradation model, which defines the relationship between *DOD* and the number of cycles to failure. The life of the battery charge and discharge cycle (N_{cycle}) is expressed as

$$N_{cycle} = \sum_{i=1}^{m} \alpha_i \times D_{DOD}, \tag{5}$$

where α_i is the constant term of the energy storage fitting curve; D_{DOD} is DOD of the battery; and m is the order of the function.

Supercapacitors operate through physical ion adsorption at the electrode–electrolyte interface, avoiding, for example, degradative Faradaic reactions found in batteries. This mechanism enables exceptional cycle stability, often exceeding millions of deep discharge cycles.[14] Consequently, given a lifespan that typically surpasses the project horizon, the supercapacitor's service life is modeled using a constant for simplification. Proactive *DOD* management (0.4–0.6) prevents battery degradation due to deep discharge, ensuring optimal lifespan and cost-efficiency.

3.3 Model formulation for wind-storage system optimization

To achieve a techno-economically optimal solution, an optimization model is developed with the objective function defined as the minimization of the system's annualized comprehensive cost. The optimization model integrates the previously defined component constraints and operational strategies to determine the ideal capacity configuration and dispatch schedule.

3.3.1 Objective function

The objective function, formulated to minimize the total annualized cost, is presented as Eq. (6). It comprises the capital and operational expenditures for the lithium-ion battery bank, the supercapacitor array, and the penalty costs associated with wind power fluctuation.

$$\min C = C_{Li} + C_{SC} + C_{comp} \tag{6}$$

Here, C represents the total annual cost of the system and consists of three main components: the cost of the lithium-ion battery C_{Li}, the cost of the supercapacitor unit C_{SC}, and the opportunity cost C_{comp} associated with compensating for wind power fluctuations.

The individual costs for the lithium-ion battery and supercapacitor can be expressed as follows:

$$C_{Li} = C_{Li}^{inv} + C_{Li}^{oper} - C_{Li}^{re}, \tag{7}$$

$$C_{SC} = C_{SC}^{inv} + C_{SC}^{oper} - C_{SC}^{re}, \tag{8}$$

where the lithium-ion battery cost C_{Li} and supercapacitor cost C_{SC} are each composed of three elements: initial investment (C_{Li}^{inv},C_{SC}^{inv}), annual O&M (C_{Li}^{oper},C_{SC}^{oper}), and end-of-life residual value (C_{Li}^{re},C_{SC}^{re}).

3.3.1.1 Investment cost formulation

The total investment includes the lithium-ion battery and supercapacitor costs.

$$C_{Li}^{inv} = \left(C_{Li,P}^{inv} P_{Li} + C_{Li,E}^{inv} E_{Li}\right) \frac{r\left(1+r\right)^{Y_{Li}}}{\left(1+r\right)^{Y_{Li}} - 1} \tag{9}$$

$$C_{SC}^{inv} = \left(C_{SC,P}^{inv} P_{SC} + C_{SC,E}^{inv} E_{SC}\right) \frac{r\left(1+r\right)^{Y_{SC}}}{\left(1+r\right)^{Y_{SC}} - 1} \tag{10}$$

Here, $C_{Li,P}^{inv}$ and $C_{Li,E}^{inv}$ denote the investment cost coefficients related to the rated power and energy capacities of the lithium-ion battery, respectively. $C_{SC,P}^{inv}$ and $C_{SC,E}^{inv}$ represent the corresponding investment cost coefficients for the supercapacitor, respectively. The parameter r refers to the discount rate, while Y_{Li} and Y_{SC} denote the service lifetimes of the lithium-ion battery and supercapacitor, respectively.

3.3.1.2 Operation and management cost

O&M cost for each component is regarded as a fixed percentage of its respective investment cost in techno-economic analyses.[15] The governing equations are expressed as

$$C_{Li}^{oper} = a_{Li} C_{Li}^{inv}, \tag{11}$$

$$C_{SC}^{oper} = a_{SC} C_{SC}^{inv}, \tag{12}$$

where a_{Li} and a_{SC} are the O&M cost coefficients for the lithium-ion battery and supercapacitor in the annual O&M expense, respectively.

3.3.1.3 Energy storage equipment recovery cost

At the end of the operational life, energy storage equipment exhibits a residual value derived from its potential for recycling or material recovery, expressed as

$$C_{Li}^{re} = \left(C_{Li,P}^{inv} P_{Li} + C_{Li,E}^{inv} E_{Li} \right) \frac{b_{Li} \cdot r}{\left(1+r\right)^{Y_{Li}} - 1}, \tag{13}$$

$$C_{SC}^{re} = \left(C_{SC,P}^{inv} P_{SC} + C_{SC,E}^{inv} E_{SC} \right) \frac{b_{SC} \cdot r}{\left(1+r\right)^{Y_{SC}} - 1}, \tag{14}$$

where b_{Li} and b_{SC} denote the end-of-life residual value coefficients for the lithium-ion battery and supercapacitor, respectively.

3.3.1.4 Fluctuation penalty compensation cost

Because of the finite power and energy ratings of the HESS, large-scale wind power fluctuations are difficult to fully mitigate. This issue necessitates the dispatch of higher-cost flexibility resources, incurring an opportunity compensation cost C_{comp} to account for these additional system expenses,[6,16] as defined by

$$C_{comp} = \sum_{n=1}^{N} K_b \left(P_{posi,n} - P_{nega,n} \right). \tag{15}$$

Here, the opportunity compensation cost is calculated using the coefficient K_b, applied to the positive and negative under-compensation power values, $P_{posi,n}$ and $P_{neg,n}$, respectively, at each time step n.

3.3.2 Constraints

3.3.2.1 System power balance constraint

In this system, positive power fluctuations are absorbed by charging the HESS, while negative fluctuations are compensated by discharging the lithium-ion battery and supercapacitor.

The net HESS power at the n-th time step ($P_{HESS,n}$) is expressed as

$$P_{HESS,n} = P_{Li,n}^{ch} + P_{SC,n}^{ch} + P_{posi,n} - P_{Li,n}^{disc} - P_{SC,n}^{disc} - P_{nega,n}, \tag{16}$$

where $P_{Li,n}^{ch}$ and $P_{Li,n}^{disc}$ respectively denote the charging and discharging power setpoints of the lithium-ion battery at time step n. Similarly, $P_{SC,n}^{ch}$ and $P_{SC,n}^{disc}$ respectively denote the charging and discharging power setpoints of the supercapacitor at time step n.

3.3.2.2 Charge/discharge power limits

The net power outputs $P_{Li,n}$ and $P_{SC,n}$ at the n-th time step in the lithium-ion battery and supercapacitor, respectively, are expressed as Eq. (17), where positive indicates discharging and negative indicates charging.

$$\begin{cases} \left|P_{Li,n}\right| \le P_{Li,N} \\ \left|P_{SC,n}\right| \le P_{SC,N} \end{cases} \tag{17}$$

The parameters $P_{Li,N}$ and $P_{SC,N}$ respectively denote the maximum allowable charging and discharging power limits for each respective storage unit within the HESS.

3.3.2.3 Energy conservation constraint

SOC dynamics for the lithium-ion battery and supercapacitor are governed by their respective energy conservation equations as follows.

$$\begin{cases} E_{Li,n} = E_{Li,n-1} + P_{Li,n}\eta_{Li,cha}, & P_{Li,n} > 0 \\ E_{SC,n} = E_{SC,n-1} + P_{SC,n}\eta_{SC,cha}, & P_{SC,n} > 0 \\ E_{Li,n} = E_{Li,n-1} + P_{Li,n}\eta_{Li,disc}, & P_{Li,n} \le 0 \\ E_{SC,n} = E_{SC,n-1} + P_{SC,n}\eta_{SC,disc}, & P_{SC,n} \le 0 \end{cases} \tag{18}$$

The remaining capacities at time step n ($E_{Li,n}$ and $E_{SC,n}$) are updated from their previous states ($E_{Li,n-1}$ and $E_{SC,n-1}$) in accordance with the charged or discharged energy, adjusted by the corresponding charging ($\eta_{Li,ch}$ and $\eta_{SC,ch}$) and discharging ($\eta_{Li,disc}$ and $\eta_{SC,disc}$) efficiencies.

3.3.2.4 *SOC* operating range constraint

The *SOC* for both the lithium-ion battery $SOC_{Li,n}$ and supercapacitor $SOC_{SC,n}$ at any time step n is bounded by their respective minimum and maximum operational limits, defined as $SOC_{Li,min}$/$SOC_{Li,max}$ and $SOC_{SC,min}$/$SOC_{SC,max}$.

$$\begin{cases} SOC_{Li,min} \le SOC_{Li,n} \le SOC_{Li,max} \\ SOC_{SC,min} \le SOC_{SC,n} \le SOC_{SC,max} \end{cases} \tag{19}$$

4. Results, Analysis, and Discussion

4.1 Techno-economic analysis of system configurations

A comparative cost analysis with three hybrid energy storage configuration schemes was conducted using a representative wind power profile. [8] The model parameters used in the test are detailed in Table 1.[6] Among all schemes, Scheme 3 with the ICEEMDAN algorithm presents the most favorable economic outcome, achieving the lowest annualized cost by effectively mitigating battery degradation and reducing fluctuation penalties. On the other hand, Scheme 2 with the CEEMDAN-based algorithm demands an intermediate cost, while Scheme 1 with the EEMD-based algorithm requires the highest cost.

The MATLAB-based practical adjustment model yielded oversizing factors of $\alpha_E = 0.54$ and $\alpha_P = 0.26$ for the lithium-ion battery and $\alpha_E = 0.23$ and $\alpha_P = 0.21$ for the supercapacitor. This signifies a required practical oversizing of 54% in energy and that of 26% in power for the battery to address operational constraints like *DOD* limits, conversion losses, and degradation. The battery's high energy oversizing factor reflects the comprehensive nature of this model compared with prior empirical approaches. Conversely, the supercapacitor's resilience allowed for substantially smaller margins. The comparative outcomes using three HESS decomposition

Table 1
Parameters for the HESS capacity optimization model.

Parameter	Value
Lithium-ion battery energy capital cost ($C^{inv}_{Li,E}$) [CNY/(kWh)]	100
Lithium-ion battery power capital cost ($C^{inv}_{Li,P}$) [CNY/(kWh)]	150
Supercapacitor energy capital cost ($C^{inv}_{SC,E}$) [CNY/(kWh)]	600
Supercapacitor power capital cost ($C^{inv}_{SC,P}$) [CNY/(kWh)]	100
Lithium-ion battery SOC operating range	[0.2, 0.8]
Supercapacitor SOC operating range	[0.1, 0.9]
Discount rate r	5%
Lithium-ion battery operational lifetime Y_{Li}/year	5
Supercapacitor operational lifetime Y_{SC}/year	15
Lithium-ion battery O&M cost factor (a_{Li})	2%
Supercapacitor O&M cost factor (a_{SC})	2%
Lithium-ion battery residual value coefficient (b_{Li})	10%
Supercapacitor residual value coefficient (b_{SC})	20%
Opportunity compensation cost coefficient (C_{comp}) [CNY/(kWh)]	0.32

schemes, detailing both the practical system configuration and the associated cost evaluation, are summarized in Table 2. Here, each scheme represents a distinct system sizing derived from its respective energy decomposition methodology.

Among all schemes, Scheme 1 (EEMD) presents a moderate battery rating (48.8 kW, 189.1 kWh). Scheme 2 (CEEMDAN) necessitates the largest battery system (88.26 kW, 251.52 kWh), whereas Scheme 3 (ICEEMDAN) achieves the most compact battery design (39.96 kW, 199.63 kWh). However, the supercapacitor power rating remains consistently high across all schemes (approximately 930–940 kW) in managing high-frequency power transients.

From an economic perspective, Scheme 2 incurs the highest lithium battery investment cost (88.67 k CNY) owing to its larger capacity, compared with 60.58 k CNY and 59.95 k CNY for Schemes 1 and 3, respectively. On the other hand, the supercapacitor investment constitutes the dominant portion of the total system cost (around 200 k CNY for all schemes), unveiling its critical importance in the power smoothing process. In O&M cost, Scheme 2 has the highest residual value corresponding to its greater installed energy capacity.

A key financial metric in the opportunity compensation cost (reflecting penalties for unsuppressed fluctuations), Scheme 2 provides the most favorable outcome, i.e., −83.35 k CNY. This suggests that the CEEMDAN algorithm can achieve superior grid stabilization, leading to higher economic benefits from quality compliance. However, substantial capital investment is demanded, where Scheme 2 requires the highest annualized cost (190.10 k CNY) and Scheme 3 has the lowest total annualized cost of 172.25 k CNY. In conclusion, these results confirm that ICEEMDAN can strike an optimal techno-economic balance. This means that a capital expenditure can be effectively minimized through a more compact battery design without paying significant penalties in practical HESS applications.

4.2 Dynamic system operation and state analysis

Using a representative wind power profile (Typical Day 2), we evaluate the proposed HESS control strategies by analyzing the power fluctuation suppression and the corresponding operational impact on storage components. The proposed decomposition-driven power split

Table 2
Techno-economic results of HESS configuration schemes.

Parameter	Scheme 1	Scheme 2	Scheme 3
System configuration			
Lithium battery power (kW)	48.797	88.264	39.956
Lithium battery capacity (kWh)	189.068	251.516	199.634
Supercapacitor power (kW)	935.624	928.91	941.39
Supercapacitor capacity (kWh)	192.821	200.885	176.301
Cost breakdown (k CNY)			
Lithium battery investment cost/k CNY	60.57625	88.67399	59.95366
Supercapacitor investment cost/k CNY	201.60105	205.61564	192.60712
Operation & Maintenance (O&M) Cost/k CNY	5.24354	5.885792	5.05121
Residual value/k CNY	24.13993	26.72760	23.22595
Opportunity compensation penalty cost /k CNY	−34.12136	−83.35247	−62.13975
Total annualized cost/k CNY	209.15956	190.09534	172.24629

simplifies hardware integration by assigning each storage device a distinct operational role. By isolating high-frequency transients to the supercapacitor, current spikes and converter stress are reduced, while allocating low-frequency power to the battery prevents rapid *SOC* fluctuations. This structured approach mitigates compatibility issues like voltage mismatch and dynamic coupling. The stabilization of wind power fluctuations using weighted filtering is shown in Fig. 3. The fundamental smoothing capability is demonstrated, contrasting the volatile original wind power with the stabilized grid-connected output (red curve).[8] Here, the performance target to improve power distribution efficiency is achieved using the advanced decomposition techniques developed in this work.

Under the EEMD-based scheme operation the battery undergoes frequent, high-amplitude charge-discharge cycles, as shown in Fig. 4. This pattern exhibits inadequate frequency separation and significant mode mixing, forcing the battery to manage short-term transient situations. Therefore, the supercapacitor cannot fully absorb the power, thereby increasing its degradation stress.

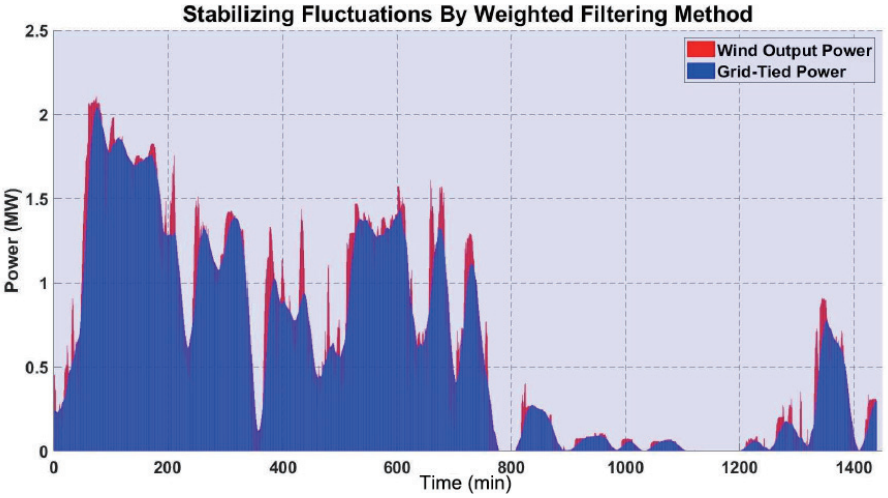

Fig. 3. (Color online) Stabilization of wind power fluctuations by weighted filtering.

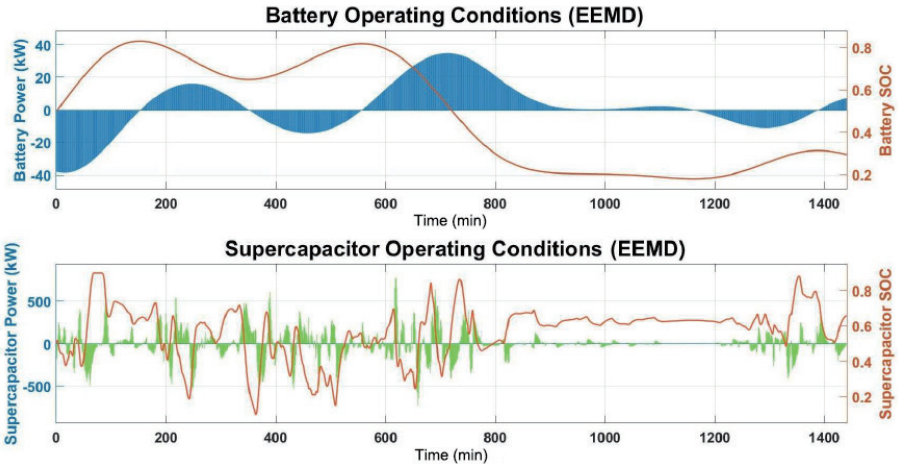

Fig. 4. (Color online) Energy storage system operating states with EEMD-based scheme.

The CEEMDAN-based scheme performance outcome, as shown in Fig. 5, indicates improved component coordination. The battery profile is notably smoother, indicating a more effective division of labor where the supercapacitor assumes a greater share of rapid power fluctuations. This reduces the battery's cycling burden under persistent power variation, although minor residual noise in the decomposition leads to slight deviations in power allocation.

The ICEEMDAN scheme performance outcome shown in Fig. 6 shows that it achieves the most effective power allocation. The battery operates with minimal, low-frequency variations, consistent with its intended role for energy management, while the supercapacitor provides rapid and precise compensation for high-frequency transients. This confirms that this optimized cooperation minimizes unnecessary battery cycling so that system stability is enhanced.

The *DOD* distribution that directly expresses the operational stress of the lithium-ion battery under the three allocation strategies is shown in Fig. 7. The EEMD-based strategy exhibits a wide *DOD* spread with significant high-level (0.7–0.8) occurrences, indicating frequent deep

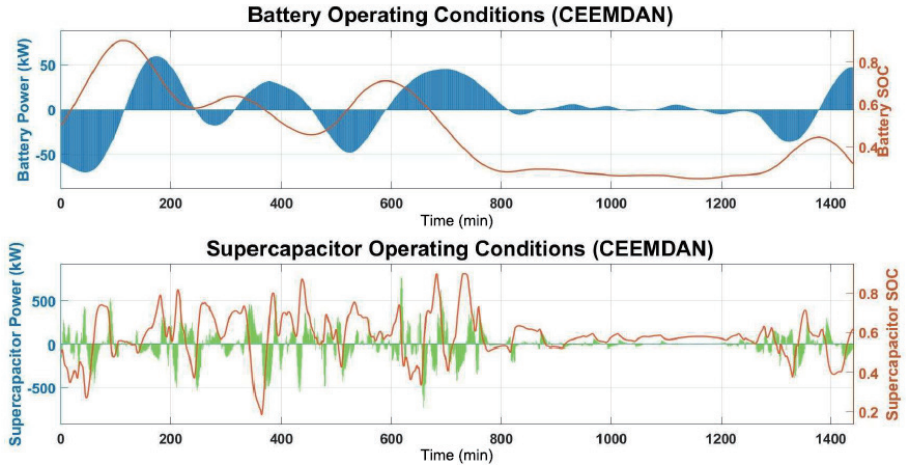

Fig. 5. (Color online) Energy storage system operating states with CEEMDAN-based scheme.

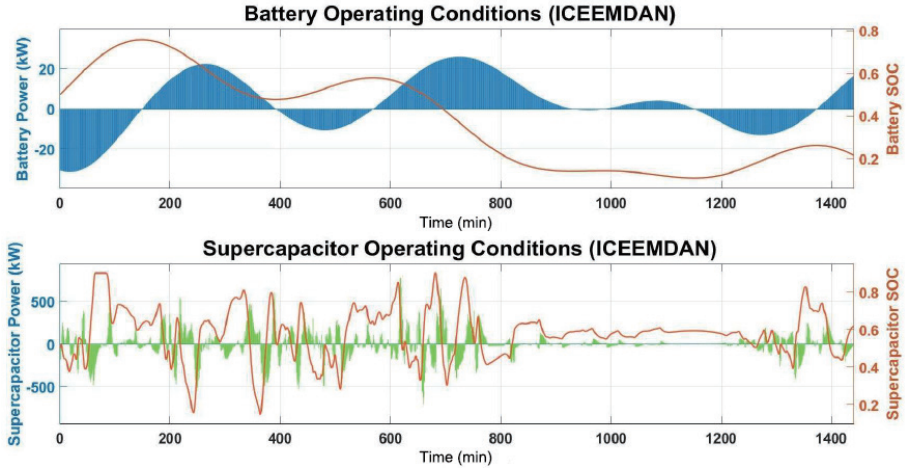

Fig. 6. (Color online) Energy storage system operating states with ICEEMDAN scheme.

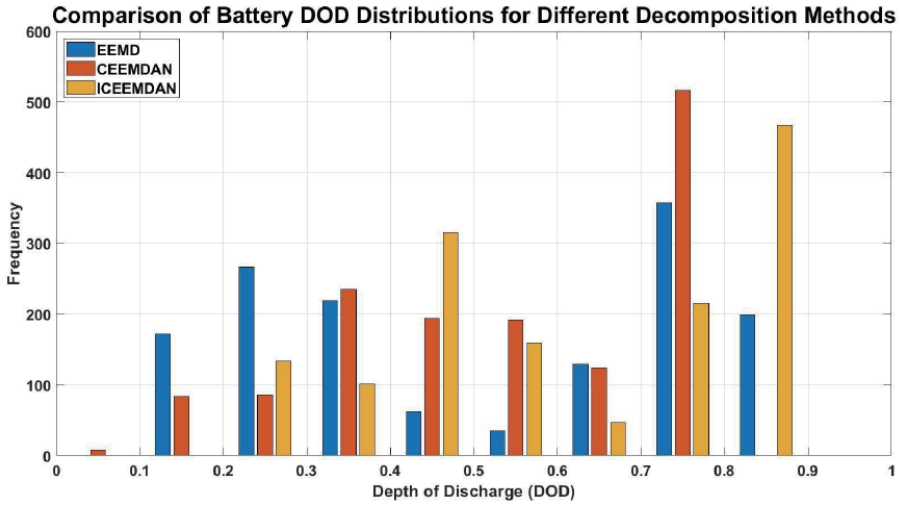

Fig. 7. (Color online) Battery DOD distributions for the three decomposition methods

cycles due to poor frequency decoupling and elevated degradation risk. The CEEMDAN-based approach shows improvement, concentrating cycles at around 0.7 *DOD* with fewer deep discharges (>0.8), signifying better mode separation. However, its persistent stress with a moderately high *DOD* has residual mode overlap and continued battery cycling burden. Compared with the above two schemes, the ICEEMDAN-based strategy presents the most favorable *DOD* profile, with cycles heavily concentrated in the moderate 0.4–0.6 range and minimal extreme discharges. This optimal distribution confirms highly efficient energy partitioning. Also, the battery predominantly manages stable, low-frequency power, thereby operating within a shallower and less stressful *DOD* range.

5. Conclusions

The results of this study demonstrate that the ICEEMDAN-based HESS model has achieved optimal techno-economic performance, yielding the lowest annualized cost (172.25 k CNY) among three evaluated decomposition algorithms. Through superior frequency separation, the proposed strategy enables the coordination of essential system components: the supercapacitor handles high-frequency transients, while the battery manages low-frequency components with minimal stress. The ICEEMDAN operational advantage was quantified by the rain flow counting method, confirming that ICEEMDAN exhibits the most favorable battery *DOD* distribution for maximizing battery longevity in the moderate 0.4–0.6 range. Moreover, for example, the total annualized cost can be reduced by 9.4 and 17.7% compared with the CEEMDAN and EEMD schemes, respectively. Consequently, ICEEMDAN emerges as the recommended approach for practical wind-storage systems, effectively balancing performance degradation concerns with economic viability.

Acknowledgments

This study was supported by the Science Tianjin Carbon Peak and Carbon Neutrality Technology Major Project (Grant no. 24ZXTKSN00030).

References

1 M. Khalid: Energies **12** (2019) 4559. https://doi.org/10.3390/en12234559
2 R. Hou, J. Liu, W. Chen, and J. Liu: J. Energy. Storage **111** (2025) 115392. https://doi.org/10.1016/j.est.2025.115392
3 M. A. Escalante. Soberanis, T. Mithrush, A. Bassam, and W. Mérida: Renew. Energy **115** (2018) 547 https://doi.org/10.1016/j.renene.2017.08.082
4 P. Roy, J. B. He, and Y. Liao: IEEE Energy Convers. Conf. Expo. (ECCE) (2020) 561–568. https://doi.org/10.1109/ECCE44975.2020.9236055
5 T. Sathiyanarayanan and D. Vijay M: Power Systems Operation with 100% Renewable Energy Sources, S. Chenniappan, S. Padmanaban, and S. Palanisamy, Eds. (Elsevier, 2024) pp. 55–64. https://doi.org/10.1016/B978-0-443-15578-9.00007-8
6 X. Zhang, L. Kang, X. Wang, Y. Liu, and S. Huang: Energies. **18** (2025) 795. https://doi.org/10.3390/en18040795
7 J. Y. Wu, S. Lan, S. J. Xiao, and Y. B. Yuan: IEEE Access. **9** (2021) 42226. https://doi.org/10.1109/ACCESS.2021.3062703
8 M. N. Shahzad, O. ur. Rahman, H. C. Lin, A. Hussain, and L. L. Li: Sens. Mater. **37** (2025) 2949. https://doi.org/10.18494/SAM5708
9 Z. Dong, Z. Zhang, Z. Li, X. Li, J. Qin, C. Liang, M. Han, Y. Yin, J. Bai, and C. Wang: Symmetry **14** (2022) 1085. https://doi.org/10.3390/sym14061085
10 S. Lei, Y. He, J. Zhang, and K. Deng: Optimal Configuration of Hybrid Energy Storage Capacity in a Microgrid Based on Variational Mode Decomposition. Energies **16** (2023) 4307. https://doi.org/10.3390/en16114307
11 C. Xu, W. Qiu, L. Si, T. Zhang, J. Li, G. Chen, H. Yu, J. Lu, and Z. Lin: Energies **16** (2023) 6621. https://doi.org/10.3390/en16186621
12 M. Matsuishi and T. Endo: Proc. Japan Society of Mechanical Engineers (1968).
13 X. Han, M. Ouyang, L. Lu, and J. Li: Appl. Energy **113** (2014) 812. https://doi.org/10.1016/j.apenergy.2013.08.015
14 X. Xiong, R. Yang, Y. Lin, and J. Li: Trans. China. Electro. tech. Soc. **28** (2013) 224 (in Chinese). https://dgjsxb.ces-transaction.com/CN/abstract/abstract2053.shtml
15 S. Khan, A. Javed, M. Muyeen, and A. Almutairi: Energy Rep. **8** (2022) 3082. https://doi.org/10.1016/j.egyr.2022.01.015
16 T. Yang, S. Lou, X. Zhang, X. Tian, and Z. Bai: Proc. 5th Int. Conf. Electric Utility Deregulation and Restructuring and Power Technologies (DRPT), Changsha, China (2015) 1935–1941. https://doi.org/10.1109/DRPT.2015.7432590

About the Authors

Muhammad Nouman Shahzad is a Ph.D. student at Hebei University of Technology in the electrical engineering department. He received his B.S. degree in electronic engineering from International Islamic University, Islamabad, Pakistan, and M.S. degree in electrical engineering from North China Electric Power University, Beijing, China. His research interests include hybrid energy storage systems, renewable energy grid integration, and control algorithms. (noumanshahzad45@gmail.com)

Obaid ur Rahman received his B.S. degree, in electronics from University of Swat, KPK, Pakistan, in 2021. He is currently pursuing an M.S. degree in electrical engineering at Hebei University of Technology, Tianjin, China. His research area focuses on renewable energy, particularly in solar energy, wind energy, and battery storage systems. (Coax1432@gmail.com)

Hsiung-Cheng Lin graduated from National Taiwan Normal University with a Bachelor's degree in 1986, Taiwan. He received his M.S. and Ph.D. degrees from Swinburne University of Technology, Australia, in 1995 and 2002, respectively. From 2011 to 2019, he was a recipient of a special talent reward from the National Science Council, Taiwan. He is currently a full professor in the Department of Electronic Engineering at National Chin-Yi University of Technology. (hclin@ncut.edu.tw)

Ling-ling Li received her M.S. degree in control theory and control engineering in 2001 and her Ph.D. degree in electrical machinery and appliances in 2004 from Hebei University of Technology. She is currently a professor at the School of Electrical Engineering, Hebei University of Technology, and a permanent member of the State Key Laboratory of Reliability and Intelligence of Electrical Equipment. Her research interests include power systems, new energy, and electrical reliability.
(lilingling@hebut.edu.cn)